Available online at www.sciencedirect.com

ScienceDirect

Microelectronic Engineering 84 (2007) 368–374

MICROELECTRONIC ENGINEERING

www.elsevier.com/locate/mee

# Study of factors affecting the hardness of ball bonds in copper wire bonding

Z.W. Zhong [a,*], H.M. Ho [b], Y.C. Tan [c], W.C. Tan [a], H.M. Goh [b], B.H. Toh [c], J. Tan [d]

[a] School of Mechanical and Aerospace Engineering, Nanyang Technological University, 50 Nanyang Avenue, Singapore 639798, Republic of Singapore
[b] Kulicke and Soffa (S.E.A.) Pte. Ltd, Block 5002, Ang Mo Kio Ave 5, #04-05, Singapore 569871, Republic of Singapore
[c] Kulicke and Soffa Pte. Ltd., 6, Serangoon North Ave 5, #03-16, Singapore 554910, Republic of Singapore
[d] Infineon Technologies Asia Pacific Pte Ltd, 168 Kallang Way, Singapore 349253, Republic of Singapore

Received 3 August 2006; received in revised form 6 November 2006; accepted 14 November 2006
Available online 11 December 2006

## Abstract

Copper wire bonding has gained popularity due to its economic advantage and superior electrical performance. However, copper is harder than gold, and replacing gold wire with copper wire introduces hardness related issues. This article reports investigations of the properties including microhardness of the copper balls bonded using $\phi$25.4-μm copper wire and different combinations of electronic-flame-off (EFO) current and firing time settings with forming gas (5%$H_2$ and 95%$N_2$) as the inert cover gas. FABs with an identical diameter, obtained under different EFO firing conditions, were ball bonded with the same wire bonding parameters established using design of experiments. Microhardness tests were then performed on the cross-section of the bonded balls. The study revealed that ultrasonic generator current is the most significant factor to increase the bonded mashed ball diameter, ball shear and shear per unit area and to decrease the ball height. The microhardness of bonded copper balls is related to the EFO parameters, with FABs obtained by higher EFO current being softer. The lower hardness is attributed to the higher maximum temperature during the FAB melting state.

*Keywords:* Copper wire bonding; Electro-flame-off; Free air ball; Microhardness

## 1. Introduction

In microelectronic products, electronic packaging plays important roles such as supplying current to integrated circuit (IC) chips and distributing signals among microelectronic devices. As IC fabrication advances rapidly, electronic packaging faces new challenges [1–3]. The never-ending requirement for better electrical performance has led to significant advances in IC fabrication and electronic packaging [4–9]. Research on reliability of advanced microelectronic devices has also become more important [10,11].

Wire bonding is the most widely used interconnection technology in microelectronic packaging. The miniature demand has sparked intensive interest in ultra-thin packages [12]. The wire-loop height is a dominating parameter in reducing the thickness of ultra thin packages [13]. Copper electroplating has also become the method of choice to deposit on-chip interconnects because of the gap super-fill capability, superior material properties and low line-resistance [14].

High quality of wire bonds is vital to the performance of an IC chip. A proper bonding-quality-control system is desirable [15]. Parameter settings for successful wire bonding depend on many factors, requiring expert knowledge to optimize critical process characteristics [16]. The principal parameters such as ultrasonic generator current, bonding force, etc., can significantly affect wire-bonding quality [17].

In ultrasonic bonding, the use of ultrasound allows metals to be cold-welded [18]. The metal is first softened by the ultrasonic energy, and then the bonding force deforms the softened ball against the softened bonding pad [19]. A

---

[*] Corresponding author. Fax: +65 6791 1859.
*E-mail address:* mzwzhong@ntu.edu.sg (Z.W. Zhong).

0167-9317/$ - see front matter © 2006 Elsevier B.V. All rights reserved.
doi:10.1016/j.mee.2006.11.003

decisive factor affecting the properties of the bond is the vibrational behavior of the bonding tool called the capillary [20]. Ultra-fine-pitch wire bonding [21] requires higher stability and robustness of ultrasonic vibrations [22].

Copper and gold wires can be used for wire bonding. Al–Si wires are also used for interconnection in microelectronic devices [23]. Gold wire is more commonly used because it does not oxidize readily. However, copper wire bonding is gaining popularity [24]. A transition from Al to Cu metallization is also in progress to improve the performance of advanced ICs [25]. Copper wire is better than gold wire in terms of production cost, electrical conductivity, and resistance to wire sweep [26]. However, copper wire has not been widely used due to its poor bondability caused by surface oxidation [27].

Copper wire bonding has bigger challenges than gold wire bonding. Strain hardening of copper during bonding makes it more difficult to be bonded on any surface [28,29]. Bonding copper wires onto a copper bond-pad surface is difficult because of the high tendency of the Cu metallization to oxidize. Less information exists for bonds using Cu wire on Al cap and less is known about the intermetallic formation on the Cu–Al interface [26].

Studies found that copper free air balls (FABs) formed in elevated shield gas with a temperature of 175 °C are softer than those formed in room-temperature shield gas [30]. Various FAB parameters affect the mechanical properties of gold FABs [31,32]. It is also necessary to study the effects of these parameters on copper FABs. Copper work hardens when it is compressed [33] and it exhibits a larger strain hardening effect at a higher strain rate [34].

## 2. Experiments

A cherry pit bonding process [35] was used to ensure that the FABs obtained were only spherical balls. Forming gas (95%$N_2$ and 5%$H_2$) was used to prevent copper oxidation and to prevent oxygen from dissolving into the copper during melting, which might lead to hardening of the copper ball. The targeted FAB diameter was 46.5 μm.

Optimum ball-bond parameters were obtained using the DOE shown in Table 1 to ensure that a bonding process window was established instead of a single point process. EFO current was 120 mA and EFO firing time was 206 μs. Ultrasonic generator (USG) current setting, contact velocity (CV) and bond force (BF) were the DOE factors and the bonded mashed ball diameter (MBD), ball height and ball shear were the bonding responses, where 1 gf = 9.8 mN.

Different combinations of EFO current and firing time settings were used to obtain the same FAB diameter of 46.5 μm. These FABs with the same size, obtained under different firing conditions with a range of low to high EFO current, were ball bonded with the same ball bond parameters. The bonded devices were then mounted in epoxy resin, cross-sectioned in the normal metallographic manner [6] along the longitudinal direction, and polished with diamond suspensions of 6, 3 and 1 μm in size.

Table 1
Details of the ultrasonic generator (USG) current setting, contact velocity (CV) and bond force (BF), and the bonding responses (mashed ball diameter (MBD), ball height and ball shear)

| Run No. | CV (μm/ms) | USG (mA) | BF (gf) | MBD (μm) | Height (μm) | Shear (gf) |
|---|---|---|---|---|---|---|
| 1 | 9.65 | 93 | 35 | 52.8 | 18.9 | 23.9 |
| 2 | 7.62 | 85 | 30 | 50.9 | 20.5 | 21.5 |
| 3 | 11.43 | 85 | 30 | 50.8 | 20.0 | 20.4 |
| 4 | 9.65 | 85 | 35 | 51.8 | 19.7 | 23.3 |
| 5 | 7.62 | 100 | 30 | 52.2 | 18.4 | 26.8 |
| 6 | 11.43 | 100 | 30 | 52.5 | 18.7 | 24.1 |
| 7 | 9.65 | 93 | 35 | 52.8 | 19.4 | 23.0 |
| 8 | 7.62 | 85 | 40 | 52.3 | 18.1 | 23.7 |
| 9 | 11.43 | 85 | 40 | 53.3 | 17.8 | 23.8 |
| 10 | 9.65 | 100 | 35 | 53.6 | 18.1 | 26.7 |
| 11 | 7.62 | 100 | 40 | 54.4 | 17.6 | 27.0 |
| 12 | 11.43 | 100 | 40 | 54.2 | 17.6 | 26.9 |
| 13 | 9.65 | 93 | 35 | 52.4 | 18.6 | 23.4 |
| 14 | 9.65 | 80 | 35 | 50.7 | 19.1 | 21.5 |
| 15 | 9.65 | 75 | 35 | 50.6 | 19.5 | 18.4 |
| 16 | 9.65 | 70 | 35 | 50.1 | 20.5 | 16.5 |
| 17 | 9.65 | 90 | 35 | 52.0 | 18.8 | 22.7 |
| 18 | 9.65 | 95 | 35 | 52.5 | 18.7 | 24.2 |

Vickers hardness measurements were performed along the length of the polished cross-section of the bonded balls using a Fischerscope HP100C hardness tester with a Vickers indenter by applying a 10-mN load with a dwell time of 5 s. The Vickers hardness of a material can be defined as the resistance of the material to permanent deformation [36]. The test uses a pointed diamond indenter and presses it into the surface of the material to be tested. To ensure accurate measurement of the hardness, indentations were measured in a JEOL 6360A SEM (scanning electron microscope). Vickers hardness values were calculated using the following formula [37]:

$$\text{Vickers Hardness (HV)} = 1.854\ (F/D^2) \qquad (1)$$

where $F$ is the applied load of the indenter with a unit of kg-f, and $D^2$ is the area of the indentation with a unit of $\text{mm}^2$.

## 3. Results and discussion

The behaviour of a bonded gold ball and its heat affected zone depend very much on the characteristics of FAB formation [31], which is affected by the EFO parameter settings, mainly the EFO current level and its corresponding firing time.

For copper wire bonding, there is a need to get the FAB properties to that of gold FABs as close as possible, because most bond-pad structures are developed to suit the nature of gold wire bonding.

### *3.1. Bonding responses*

Copper wiring bonding was conducted according to Table 1. Measurements with a sample size of 16 were carried out to obtain the average values of MBD, ball height and ball shear, and the results are also shown in Table 1. Analysis of the results revealed that the increase in ultrasonic generator current and bond force would result in increased MBD and decreased ball height, while contact velocity had little effect on these two responses. Increase in ultrasonic generator current would increase ball shear but increase in contact velocity would reduce this response.

The experiments did not produce any NSOP (non-sticking on pad) defect with any of the parameter settings in Table 1. A process window was formed with a contact velocity of 9.65 μm/ms and a bond force of 35 gf as the constant settings.

### 3.2. Effects of USG current

Figs. 1 and 2 show the effects of ultrasonic generator current on MBD, ball height, ball shear and shear per unit area. The MBD and the ball shear increased but the ball height decreased with increased ultrasonic generator current. The shear per unit area initially increased, got saturated over a range and then increased again, when the ultrasonic generator current increased.

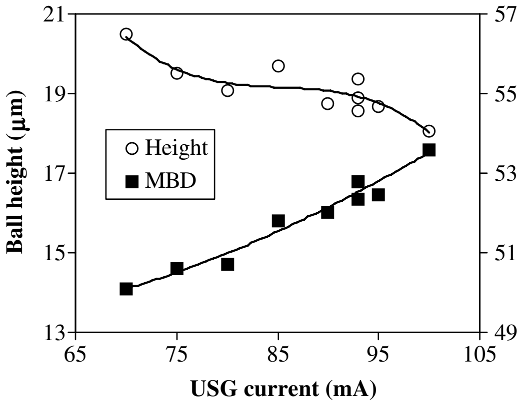

Fig. 1. Effects of ultrasonic generator (USG) current on MBD and ball height.

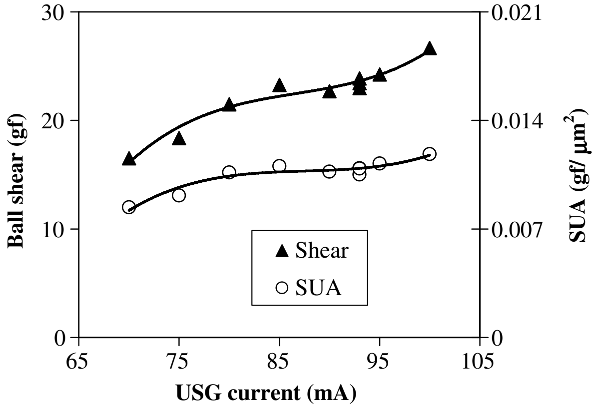

Fig. 2. Effects of ultrasonic generator (USG) current on ball shear and shear per unit area (SUA).

The shear per unit area represents how well the weld between the copper and its aluminium bond pad of an IC chip has been formed. Fig. 2 suggests that there could be an optimum ultrasonic generator current setting in the region of saturation of shear per unit area. Higher shear per unit area could be achieved by using higher ultrasonic generator current, but this might cause cratering on the aluminium bond pad of the IC chip.

### 3.3. Effects of EFO current and firing time

Table 2 shows FAB sizes obtained using three EFO current and firing time settings. The settings resulted in average FAB sizes that were close to the required FAB size of 46.5 μm.

Fig. 3 shows the bonded MBDs and bonded ball heights obtained using three ultrasonic generator (USG) current settings (70, 90 and 100 mA) and the FABs formed using the three (high, medium and low) EFO current settings, and Fig. 4 shows the corresponding ball shear and shear per unit area (SUA). In these figures, at each USG current level for each response (size, height, shear or SUA), there are three data indicating the responses corresponding to the three EFO current settings.

As shown in Figs. 3 and 4, the three USG current settings (70, 90 and 100 mA) had more significant effects on the responses than the three (high, medium and low)

Table 2
Average FAB sizes obtained using three EFO current and firing time settings

| EFO ID | EFO current (mA) | Firing time (μs) | FAB size (μm) |
|---|---|---|---|
| High | 105 | 243 | 46.73 |
| Medium | 60 | 476 | 46.54 |
| Low | 30 | 1248 | 46.55 |

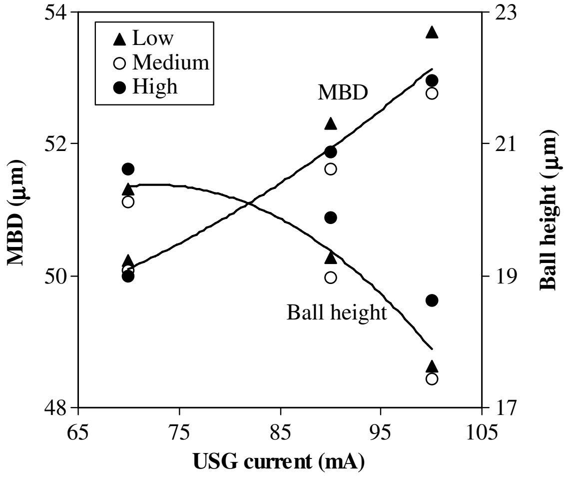

Fig. 3. Bonded MBDs and bonded ball heights obtained using three ultrasonic generator (USG) current settings (70, 90 and 100 mA) and the FABs formed using the three (high, medium and low) EFO current settings.

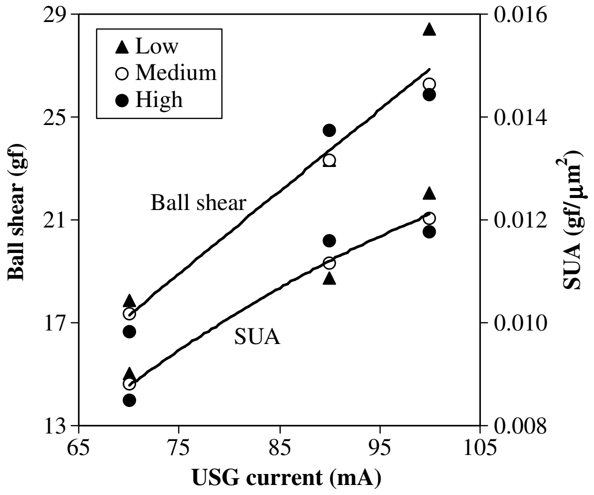

Fig. 4. Ball shear and shear per unit area (SUA) of the ball bonds obtained using three ultrasonic generator (USG) current settings (70, 90 and 100 mA) and the FABs formed using the three (high, medium and low) EFO current settings.

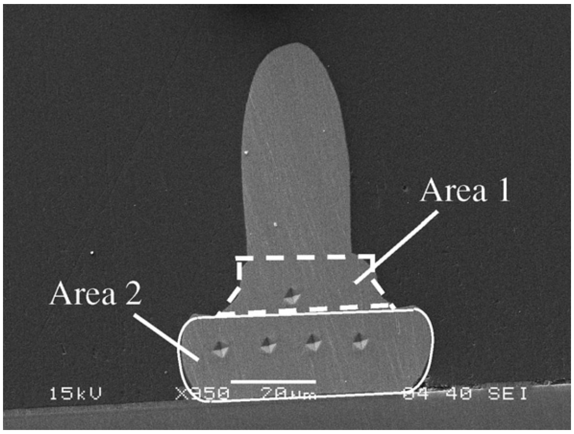

Fig. 5. Indentation locations for microhardness tests.

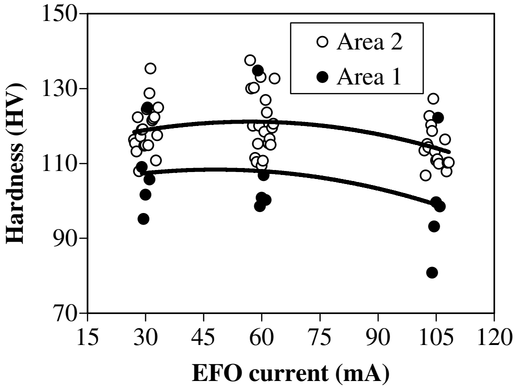

Fig. 6. Vickers hardness numbers (HV) of the ball bonds obtained using ultrasonic generator current = 90 mA, contact velocity = 7.62 μm/ms and the FABs formed using the three (high, medium and low) EFO current settings shown in Table 2.

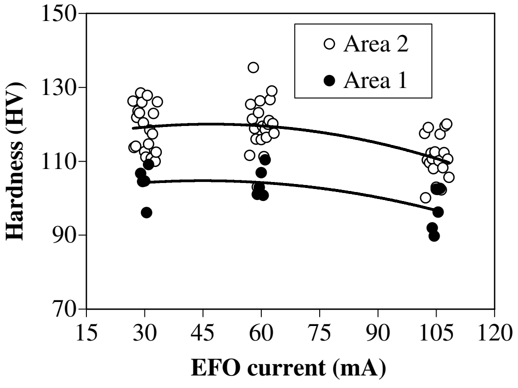

Fig. 7. Vickers hardness numbers (HV) of the ball bonds obtained using ultrasonic generator current = 90 mA, contact velocity = 11.43 μm/ms and the FABs formed using the three (high, medium and low) EFO current settings shown in Table 2.

EFO current settings. Optical measurement of the ball bonds and the shear measurement method could only distinguish the differences made by the USG current settings but not that made by the three EFO current settings. There was a need to employ a measuring method with higher resolution to quantify the effects of different EFO current levels. This led to the use of Vickers hardness test, which is reported in Section 3.4.

After the FAB has been squashed to the shape of the ball bond by the initial contact velocity, the weld is formed by application of ultrasonic and thermal energies together with bonding force. The ultrasonic energy reduces the yield stress of the copper ball and at the same time helps to form the weld at the interface. Once a good weld is formed, there should be no displacement at the interface, because it will degrade the weld. As shown by Figs. 3 and 4, higher ultrasonic generator current resulted in more deformed ball bonds and good welds with higher ball shear and shear per unit area, with the process parameter settings investigated.

### *3.4. Vickers hardness of ball bonds*

Vickers hardness tests were conducted to quantify the effects of different EFO current levels on the microhardness of the ball bonds. Fig. 5 illustrates an example of indentations performed on the inner-chamfer area of the bonding tool (Area 1, outlined in white broken lines) and the smashed ball area (Area 2, outlined in white solid lines).

Figs. 6 and 7 show the Vickers hardness numbers (HV) of the ball bonds obtained using ultrasonic generator current = 90 mA, contact velocity = 7.62 and 11.43 μm/ms, respectively, and using the FABs formed using the three (high, medium and low) EFO current settings shown in Table 2. The average numbers of the Vickers hardness of bonded balls formed at higher EFO current are lower than those formed at lower EFO current. The average Vickers hardness on the inner-chamfer area of the bonding tool (Area 1) is slightly lower than that of the smashed ball area (Area 2).

There were measurement errors, which were inherent to the hardness test and were included in the hardness values shown in Figs. 6 and 7. Therefore, two *t*-tests were applied to the results in Figs. 6 and 7 to statistically compare the hardness values of Area 2 obtained with high EFO current to those obtained with medium EFO current. The test applied to the results in Fig. 6 revealed that there actually was a highly significant difference ($P\text{-value} = 0.008$) between the mean (114.26 HV) of the hardness values obtained with high EFO current and that (120.82 HV) obtained with medium EFO current. The estimated difference was 6.56 HV. The test applied to the results in Fig. 7 revealed that there actually was a very highly significant difference ($P\text{-value} < 0.001$) between the mean (110.55 HV) of the hardness values obtained with high EFO current and that (119.83 HV) obtained with medium EFO current. The estimated difference was 9.28 HV. As also shown in Fig. 3, the processes with various EFO currents resulted in different mashed (deformed) ball dimensions, which resulted in different work-hardening levels and thus affected the Area-2 hardness values of the processes with various EFO currents.

The smashed ball area (Area 2) was expected to have higher hardness than the inner-chamfer area of the bonding tool (Area 1), because it experienced more strain hardening [28].

The *t*-test applied to the results in Fig. 7 confirmed that the Vickers hardness of the balls bonded using FABs formed at 105-mA EFO current was lower than that formed at 60-mA EFO current, with a difference of approximately 10 HV. Because all parameters were constant except for the EFO firing conditions, it is reasonable to deduce that the hardness decrease on the bonded balls is attributed to the deformed ball dimensions, which resulted from the higher EFO current setting.

To visualize the effect of the 10-HV hardness difference, it is better to express it in terms of yield stress. A semi-empirical relationship between HV and yield stress $\sigma_{0.2}$ was proposed to be [29]:

$$\sigma_{0.2} = 3.27\,\mathrm{HV}(0.1)^n \qquad (2)$$

where $n$ is a strain-hardening index.

This semi-empirical relationship indicates that the lower the hardness (HV), the lower will be the yield stress ($\sigma_{0.2}$). This relationship enables the estimation of the yield stress ratio by simply taking the ratio of hardness (HV) and assuming that n is a constant. The calculation using the ratio of hardness numbers for FABs formed at 60 mA and 105 mA revealed a 9% reduction in yield stress. This has the implication that the stress experienced on the bond pad is lower when it is bonded with the copper FAB formed at 105-mA EFO current compared with that formed at 60 mA.

### 3.5. *FABs formed by "high" EFO current*

The copper FAB formed by "high" EFO current is a relative term, because it also heavily depends on the copper wire diameter used. EFO current of 105 mA can be considered high for forming FABs using a copper wire diameter of 25.4 μm, but this could be low for forming FABs using a copper wire diameter of 50.8 μm. Therefore, using EFO current as a standard index is not appropriate.

Fig. 8 shows the EFO firing conditions for obtaining a FAB diameter of 46.5 μm with 25.4-μm (1 mil) wire and obtaining a FAB diameter of 93 μm with 50.8-μm (2 mil) wire. 120 mA is "high" EFO current for 25.4-μm (1 mil) copper wire, but it is regarded as "low" for 50.8-μm (2 mil) copper wire.

For gold wire bonding, it has been shown numerically that higher EFO current would result in higher maximum FAB temperature [31]. It is deemed that the same mechanism works for copper FABs, and it is the higher temperature that contributes to the lower hardness, during FAB formation using higher EFO current.

During copper FAB formation, if the inert-gas is insufficient to provide totally volumetric coverage, oxidation will take place during melting of the wire tail [38]. This will result in a pointed FAB, because the surface tension will significantly decrease due to oxidation of the surface layer of the molten copper FAB [39].

An experiment using $\phi$50.8-μm copper wire was performed to confirm that a higher EFO current tends to result in a higher temperature during FAB formation. The experiment was the typical cherry pits bonding. Copper FABs having the same diameter were obtained using different combinations of EFO current and firing time settings at a low flow rate (1.0 scfh) of forming gas. These FABs were then inspected using the SEM to investigate the roundness of the FABs. The results are shown in Table 3.

Fig. 9 shows SEM pictures of the cherry bond pits for the inspection of the FABs formed with 250-mA EFO current, with mixture of spherical balls and pointed balls.

As shown by Table 3, there were more non-spherical FABs formed by higher EFO current. This could be due to the following reason: During copper FAB formation, the maximum temperature of the copper ball can be very

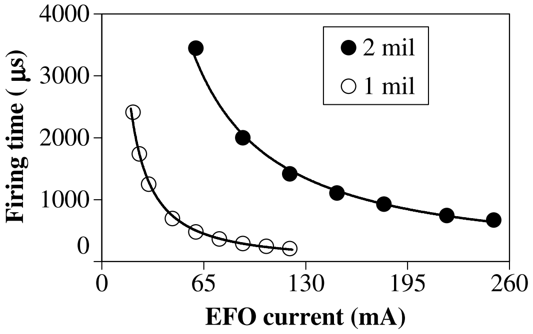

Fig. 8. EFO firing conditions for obtaining a FAB diameter of 46.5 μm with 25.4-μm (1 mil) wire and obtaining a FAB diameter of 93 μm with 50.8-μm (2 mil) wire.

Table 3
Numbers of round FABs formed using different EFO current and firing time settings

| EFO current (mA) | Firing time (μs) | FAB diameter (μm) | No. of round FABs |
|---|---|---|---|
| 250 | 700 | 94.99 | 80/100 |
| 220 | 820 | 97.79 | 98/100 |
| 180 | 1050 | 100.85 | 100/100 |
| 150 | 1200 | 97.92 | 100/100 |
| 120 | 1500 | 97.27 | 100/100 |
| 90 | 2250 | 100.42 | 100/100 |
| 60 | 3500 | 94.99 | 100/100 |

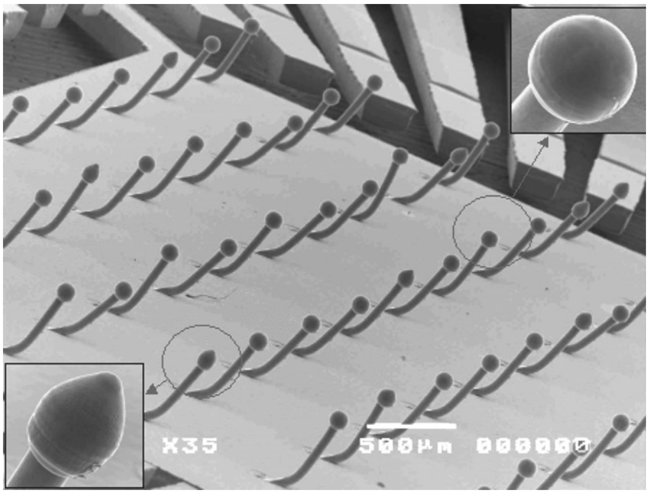

Fig. 9. SEM pictures of the cherry bond pits for the inspection of the FABs formed with 250-mA EFO current.

high. The sudden expanding in volume due to rise in temperature at the molten FAB vicinity can be several times that of the original volume. Therefore, if the flow rate is not sufficiently high to provide a complete inert gas envelope during the melting of the copper FAB, the oxygen in the surrounding air may come in and oxidization of the surface layer of the molten copper FAB takes place, resulting in a pointed FAB.

Table 3 shows that FABs formed at higher EFO current had occasional pointed balls. Hence, it is reasonable to assume that higher EFO current could result in higher temperature during the melting of FABs. This is further supported by the fact that all FABs with similar diameters formed at lower EFO current did not have pointed FABs.

Figs. 10 and 11 show the enlarged views of the SEM pictures for the pointed FAB and the spherical FAB indicated in Fig. 9, respectively. It can be seen that there was some level of scaling at the region of the pointed ball, but the spherical ball had a relatively smooth surface. The scaling was most likely due to oxidization of the surface layer of the molten copper FAB.

To have all FABs in the spherical form, to increase the flow rate of the forming gas can be another solution. This will provide volumetric coverage with sufficient inert gas during copper FAB formation.

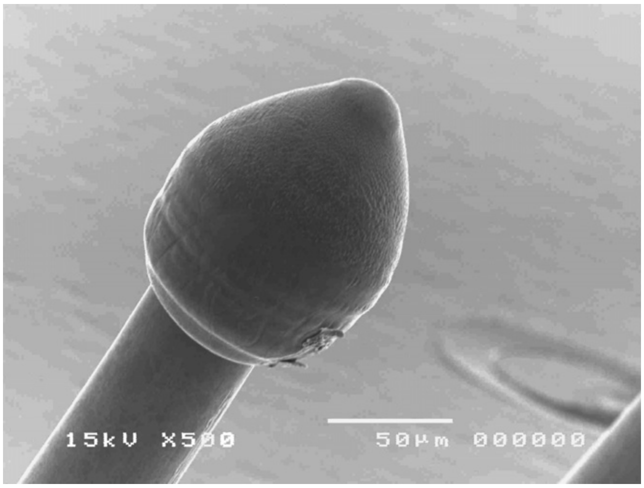

Fig. 10. SEM picture of a pointed FAB with a scaling surface.

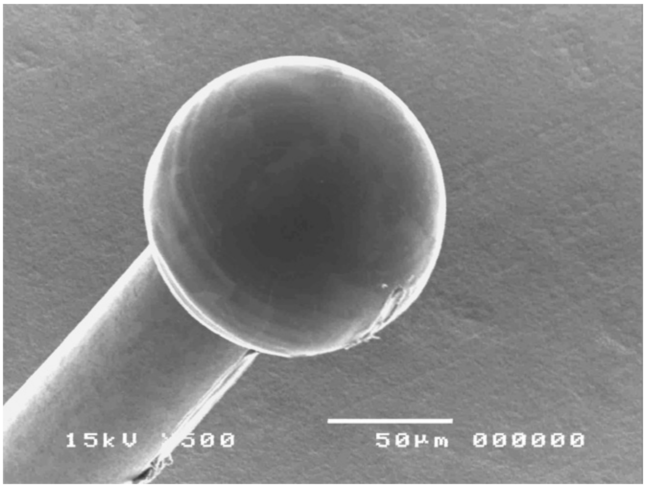

Fig. 11. SEM picture of a spherical FAB with a relatively smooth surface.

## 4. Conclusions

Ultrasonic generator current is the most significant factor to increase the bonded MBD, ball shear and shear per unit area and to decrease the ball height. The microhardness of bonded copper balls is related to the EFO parameters, with FABs obtained by higher EFO current being softer. The lower Vickers hardness is attributed to the higher maximum temperature during the FAB melting state. Higher EFO current results in a higher maximum temperature of the copper FAB. Because EFO current and firing time are closely related, it is more appropriate to use firing time as an index. This would make it less dependent on the diameter of the wire. Therefore, for copper wire bonding, to achieve a softer FAB so as to minimize the stress induced during ball bond impact, it is recommended to have shorter firing time during FAB formation, use a lower contact velocity to minimize the impact stress, and use a higher gas flow rate to provide sufficient inert-gas coverage in order to avoid pointed FABs.

## Acknowledgement

The authors would like to thank Mr. Frank Wulff for his constructive discussions and technical support on microhardness testing.

## References

[1] C.P. Wong, S. Luo, Z. Zhang, Science 290 (5500) (2000) 2269–2270.
[2] Z. Zhong, Microelectronics International 16 (3) (1999) 6–14.
[3] P. Palm, J. Maattanen, A. Picault, Y. De Maquille, Microelectronics International 18 (3) (2001) 27–31.
[4] Z. Zhong, Soldering and Surface Mount Technology 13 (2) (2001) 35–38.
[5] F. Oldervoll, F. Strisland, Microelectronics Reliability 44 (6) (2004) 1009–1015.
[6] C.D. Breach, F. Wulff, Microelectronics Reliability 44 (6) (2004) 973–981.
[7] Z. Zhong, P.K. Yip, Soldering and Surface Mount Technology 15 (1) (2003) 21–25.
[8] A. Hamidi, N. Beck, K. Thomas, E. Herr, Microelectronics Reliability 39 (6–7) (1999) 1153–1158.
[9] M. Petzold, L. Berthold, D. Katzer, H. Knoll, D. Memhard, P. Meier, K.-D. Lang, Microelectronics Reliability 40 (8–10) (2000) 1515–1520.
[10] T.Y. Tee, H.S. Ng, D. Yap, X. Baraton, Z. Zhong, Microelectronics Reliability 43 (7) (2003) 1117–1123.
[11] Y.G. Lu, Z.W. Zhong, J. Yu, H.M. Xie, B.K.A. Ngoi, J.B. Chai, A. Asundi, Review of Scientific Instruments 72 (4) (2001) 2180–2185.
[12] K. Gurnett, Microelectronics Journal 26 (7) (1994) xxiii–xxvi.
[13] K. Gurnett, Microelectronics Journal 26 (7) (1995) i–v.
[14] V.M. Dubin, Microelectronic Engineering 70 (2–4) (2003) 461–469.
[15] P.W.-P. Chu, C.-P. Chong, H.L.-W. Chan, K.M.-W. Ng, P.C.-K. Liu, Microelectronic Engineering 66 (1–4) (2003) 750–759.
[16] C.D. Kinnaird, A. Khotanzad, IEEE Transactions on Electronics Packaging Manufacturing 22 (3) (1999) 233–243.
[17] S. Kim, N. Hemati, EEP-Structural Analysis in Microelectronics and Fiber Optics 8 (1994) 31–40.
[18] L. Parrini, IEEE Transactions on Electronics Packaging Manufacturing 26 (1) (2003) 37–45.
[19] G.G. Harman, Wire Bonding in Microelectronics: Materials, Processes, Reliability, and Yield, McGraw Hill, NY, 1997.
[20] U. Draugelates, K.-H. Konig, SPIE Proceedings 2358 (1994) 506–520.
[21] Z. Zhong, K.S. Goh, Journal of Electronics Manufacturing 10 (4) (2000) 211–217.
[22] L. Parrini, IEEE Transactions on Ultrasonics, Ferroelectrics, and Frequency Control 48 (6) (2001) 1632–1639.
[23] W. Qin, R. Doyle, T. Scharr, M. Shah, M. Kottke, G. Chen, D. Theodore, Microelectronic Engineering 75 (1) (2004) 111–116.
[24] H.M. Buschbeck, European Semiconductor 26 (12) (2005) 27–30.
[25] C.M. Whelan, M. Kinsella, L. Carbonell, H.M. Ho, K. Maex, Microelectronic Engineering 70 (2–4) (2003) 551–557.
[26] P. Ratchev, S. Stoukatch, B. Swinnen, Microelectronics Reliability 46 (2006) 1315–1325.
[27] S. Kaimori, T. Nonaka, A. Mizoguchi, IEEE Transactions on Advanced Packaging 29 (2) (2006) 227–231.
[28] F.W. Wulff, C. Breach, D. Dtephan, Saraswati, K. Dittmer, M. Garnier, Further characterisation of intermetallic growth in copper and gold ball bonds on aluminium metallisation, in: Proceedings of the SEMI Technology Symposium (STS) S1 Advanced Packaging Technologies 1, Singapore, 5 May 2005, pp. 35–43.
[29] E.P.P. Saraswati, D. Theint, H.M. Stephan, E. Goh, D.R.O. Pasamanero, F.W. Calipto, C.D. Wulff, Breach, high temperature storage (HTS) performance of copper ball bonding wires, in: Proceedings of the Seventh Electronic Packaging Technology Conference, Singapore, 7–9 December 2005, pp. 602–607.
[30] J. Onuki, M. Koizumi, H. Suzuki, Journal of Applied Physics 68 (11) (1990) 5610–5614.
[31] W. Qin, I.M. Cohen, P.S. Ayyaswamy, Ball size and HAZ as functions of EFO parameters for gold bonding wire, in: Proceedings of the Pacific Rim/ASME International Intersociety Electronic and Photonic Packaging Conference, New York, 1997, pp. 391–398.
[32] J.L. Chen, Y.C. Lin, IEEE Transactions on Electronic Packaging Manufacturing 23 (2) (2000) 116–122.
[33] W.D. Callister, Materials Science and Engineering: An Introduction, John Wiley and Sons, New York, 2000.
[34] A. Bhattacharyya, D. Rittel, G. Ravichandran, Scripta Materialia 52 (2005) 657–661.
[35] J. Tan, Z.W. Zhong, H.M. Ho, Microelectronic Engineering 81 (2005) 75–82.
[36] H. Chandler, Hardness Testing, ASM International, Ohio, 1999.
[37] S. Mukerji, T. Kar, Crystal Research Technology 34 (1999) 1323–1328.
[38] H.M. Ho, J. Tan, Y.C. Tan, B.H. Toh, P. Xavier, Modelling energy transfer to copper wire for bonding in an inert environment, in: Proceedings of the Seventh Electronic Packaging Technology Conference, Singapore, 7–9 December 2005, pp. 292–297.
[39] E. Ricci, R. Novakovic, Gold Bulletin 34 (2) (2001) 41–49.